

Online-characterization of dielectric barrier discharge plasma actuators for optimized efficiency of aerodynamical flow control applications

J Kriegseis¹, D Schröter¹, S Grundmann² and C Tropea^{1,2}

¹ Institute of Fluid Mechanics and Aerodynamics,

² Center of Smart Interfaces,

Technische Universität Darmstadt, D-64287 Darmstadt, Germany

E-mail: kriegseis@sla.tu-darmstadt.de, grundmann@csi.tu-darmstadt.de

Abstract. The impact of fluctuating and transient kinematic and thermodynamic airflow conditions on the performance of dielectric barrier discharge (DBD) plasma actuators is demonstrated. A novel online-characterization and control approach is introduced, revealing the possibility of compensating for impaired discharge performance due to changing airflow scenarios during actuator operation. The goal of controlling the plasma actuator performance online and in situ is achieved and successfully demonstrated.

1. Introduction

Dielectric barrier discharge (DBD) plasma actuators have proven to be an attractive and promising control device for various aerodynamic flow-control applications, as summarized comprehensively by Moreau [1]. In the large number of recent publications on this topic it is commonly assumed that the discharge effects the flow, but not vice versa. The reports of flow-control experiments deal with free stream velocities ranging between several meters per second and supersonic conditions. In contradiction to that, mainly quiescent air experiments have been conducted to characterize actuator performance, for instance the impact of ambient conditions (e.g. temperature, pressure, humidity) or actuator-specific parameters (e.g. geometry, dielectric material) on the wall jet induced by plasma actuators.

However, very few studies quantitatively report on the electrical performance of such actuators, i.e. the discharge intensity, the power consumption and the corresponding electrical efficiency. This is a clear deficiency, since electrical performance should be the basis on which to evaluate the overall control authority of plasma actuators in flow control applications. Kriegseis *et al.* [2] suggested a new diagnostic approach for evaluating the performance of plasma actuators quantitatively, which is based on voltage-charge cyclograms. These Lissajous figures are a powerful and well-established means to quantitatively analyze dielectric barrier discharges [3,4], in the present case yielding the electrical power consumption P_A of plasma actuators.

Based on the previously reported dependency of discharge-light emission on the consumed power by Enloe *et al.* [5], Kriegseis *et al.* [6] demonstrated correlations of power consumption P_A , effective discharge capacitance C_{eff} , (chord wise) plasma length Δx and resulting thrust production F in quiescent air. First (qualitative) reports by Pavon *et al.* [7] indicated the

adverse effect of high airflow speed on the discharge intensity in terms of a reduced overall light emission. Recently, Barckmann *et al.* [8] demonstrated and quantified that power consumption and effective discharge capacitance of plasma actuators are considerably affected by changing airflow velocities.

Continuing in the direction of recent investigations [2, 6–8] the present manuscript addresses the above mentioned discrepancies with a new online diagnosis tool for DBDs. Such a monitoring system is essential for optimal flow-control using DBD plasma actuators, since it provides the required information to characterize and quantify the impact of fluctuating or transient airflow conditions on the plasma-actuator performance during operation. A quantitative measure of the performance is fundamentally important for any optimization procedure, since any plasma actuator flow-control system, which has previously been impedance matched for a particular reference Mach number and thermodynamic state, can be considerably de-tuned by simply varying the free stream velocity and/or the altitude (temperature, pressure or density). Therefore, a detailed online knowledge of the actuator's performance is essential to permanently maintain the optimum electrical efficiency and flow-control effectiveness during operation at changing airflow conditions.

2. Experimental Procedure

The experimental setup comprises two measurement systems, as sketched in Figure 1. A plasma actuator as used in [2] of $L = 0.11\text{m}$ length is mounted at the wall of the wind-tunnel's test section. At the opposite window a CMOS camera (Phantom V12.1, 512×512 pixels, 24fps; Nikon 105 mm, AF Micro NIKKOR f/2.8D) is used to record the spatio-temporal light emission of the discharge during the power-consumption analysis (cp. [6]). The electrical control circuit is built up using a digital oscilloscope (Picotech PicoScope4424, 4CHs, 2500p/Ch, 10MS/s) to record the operating voltage V (Testec HVP-15HF, 1000:1) and the voltage V_p across the charge-probe capacitor $C_p = 22\text{nF}$ (LeCroy PP006A, 10:1). The operating voltage V is generated by a high voltage generator (GBS Elektronik, Minipuls2), which is driven by a notebook-controlled laboratory power supply (Volcraft VSP 2410) and a function generator (GW Instek, SFG-2004, fixed frequency: $f = 12.0\text{ kHz}$).

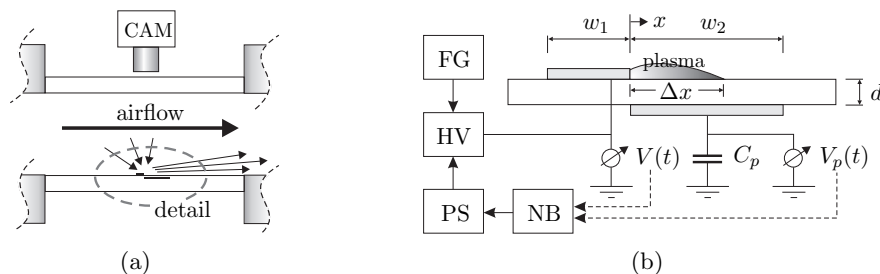


Figure 1. Sketch of experimental setup. (a) Wind tunnel test section and overhead camera (CAM); (b) detailed view of electrical plasma-actuator setup comprising function generator (FG), power supply (PS), high voltage (HV) transformer, notebook (NB) and plasma actuator.

The experiments are conducted in a blow-down type wind tunnel in order to obtain a transient airflow during experimentation, as shown in Figure 2. The static pressure p ranges between $p_{\min} = 0.89\text{ bar}$ and $p_{\max} = 1.45\text{ bar}$ during the blow-down. Benard *et al.* [9] and Versailles *et al.* [10] previously reported a favorable and adverse impact on plasma actuator performance at quiescent air conditions under reduced and elevated pressure levels, respectively.

The online-characterization of the voltage-charge cyclograms, i.e. for monitoring or controlling purposes, is based on the diagnostic approach as introduced by Kriegseis *et al.* [2].

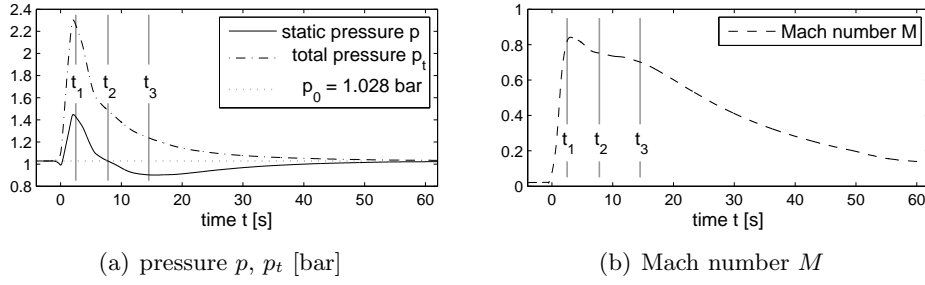


Figure 2. Transient flow conditions. (a) Static and total pressure p , p_t ; (b) Mach number M ; characteristic times are labeled as t_1 , t_2 , t_3 (cp. Table 1).

For every time step t^i the algorithm calculates the power consumption

$$P_A^i = f E^i = f \oint_{t^{i-1}}^{t^i} Q dV \quad \text{with} \quad Q = C_p V_p. \quad (1)$$

When using the diagnostic tool in closed-loop control mode, the algorithm furthermore compares P_A^i with a pre-set power level P_A^* and calculates the control signal $u^{i+1} = u^{i+1}(u^i, P_A^i, P_A^*)$ for the next time step by means of a PD control algorithm, which is then sent to the power supply (see Figure 2(b)). The light-emission data is used to validate the online-diagnostic tool by means of the temporal plasma length evolution Δx (cp. [6]).

3. Results

The pre-set initial conditions of $f = 12\text{kHz}$, $V = 10\text{kV}$ and $p_0 = 1.028$ bar result in an initial power consumption $P_A = P_A^* = 7.2\text{W}$ for $t < 0$. Three characteristic times are highlighted for $p(t_1) = p_{\max}$, $p(t_2) = p_0$, $p(t_3) = p_{\min}$ with the purpose of distinguishing pressure and air-speed effects on the discharge performance (see Figures 2 and 3).

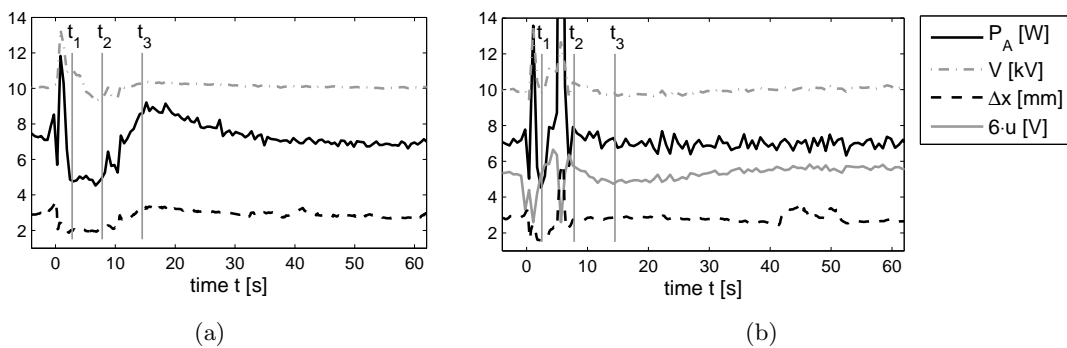


Figure 3. Results of consumed power P_A , operating voltage V , plasma length Δx and remote signal u for (a) monitoring and (b) controlling modes of operation (cp. Table 1).

The results the monitoring experiment (Figure 3(a)) clearly reveal the impact of the transient flow conditions on the resulting actuator power P_A . Immediately after the wind tunnel valve is opened at $t = 0$ a power peak occurs due to an initial expansion wave passing the test section, which is followed by a significant performance drop ($P_A = 4.8\text{W}$) once the blow-down scenario is fully developed at t_1 under adverse pressure conditions at maximum airflow speed (see Table 1). With decreasing Mach number and pressure at t_2 a constantly reduced performance

($P_A = 4.9\text{W}$) is observed, solely due to the impact of high speed airflow ($M = 0.75$) at ambient pressure conditions p_0 , which agrees with the reports of Barckmann *et al.* [8]. The influence of the minimum pressure at t_3 exceeds the adverse airflow impact ($M = 0.69$), which results in an increased performance $P_A = 8.7\text{W}$ as compared to the initial value $P_A^* = 7.2\text{W}$. Thereafter, all quantities asymptotically return to their initial values again. The plasma length Δx of the simultaneously recorded light-emissions further confirms the correctness of the online characterization of the power consumption.

Table 1. Measured data at characteristic times; ^{*m*} monitoring, ^{*c*} controlling (cp. Figure 3).

	p [bar]	M	P_A [W]	V [kV]	Δx [mm]	u [V]
$t < 0$	1.03	0	7.2 ^{<i>m,c</i>}	10.0 ^{<i>m,c</i>}	2.9 ^{<i>m,c</i>}	0.89 ^{<i>c</i>}
$t_1 = 2.4[\text{s}]$	1.45	0.84	4.8 ^{<i>m</i>} 5.7 ^{<i>c</i>}	10.8 ^{<i>m</i>} 10.1 ^{<i>c</i>}	1.9 ^{<i>m</i>} 1.6 ^{<i>c</i>}	0.97 ^{<i>c</i>}
$t_2 = 7.8[\text{s}]$	1.03	0.75	4.9 ^{<i>m</i>} 7.5 ^{<i>c</i>}	9.4 ^{<i>m</i>} 10.2 ^{<i>c</i>}	2.0 ^{<i>m</i>} 2.8 ^{<i>c</i>}	0.95 ^{<i>c</i>}
$t_3 = 14.5[\text{s}]$	0.89	0.69	8.7 ^{<i>m</i>} 7.2 ^{<i>c</i>}	10.3 ^{<i>m</i>} 9.8 ^{<i>c</i>}	3.3 ^{<i>m</i>} 2.8 ^{<i>c</i>}	0.78 ^{<i>c</i>}

For identical initial and airflow conditions the results of the closed-loop control experiment are shown in Figure 3(b). The control algorithm fails for the very strong initial power oscillation of the passing expansion wave. Thereafter the performance drop is identified at t_1 and the algorithm counter-acts this drop, as shown by the slope of the control signal u . At $t = 5.5\text{s}$ the control algorithm collapses for a single time step, which causes a power overshoot. Apart from this peak the algorithm successfully conducts a closed-loop control of the the above-discussed power variations, which again is confirmed by the results of the plasma-length Δx . Qualitatively, the slope of the remote signal u of the controlled case directly mirrors the slope of the power P_A of the uncontrolled case, which underlines the successful counter-action of the controller even in this simple proof of concept approach.

4. Conclusions

In accordance with literature, the impact of changing kinematic and thermodynamic airflow conditions on the performance of dielectric barrier discharge (DBD) plasma actuators is demonstrated. The necessity of counter-acting these performance fluctuations is met by a novel online-characterization and in-situ-control approach. Based on the measured real-time performance data, the possibility of achieving a constant plasma-actuator performance during operation under fluctuating and transient flow conditions is demonstrated in a simple proof of concept approach. This is an important insight, since beyond the common purpose of favorably manipulating the airflow, any advanced DBD-based flow control system will necessarily require an appropriate closed-loop control of the discharge device.

References

- [1] Moreau E 2007 *J. Phys. D: Appl. Phys.* **40** 605–636
- [2] Kriegseis J, Möller B, Grundmann S and Tropea C 2010 Capacitance and power consumption quantification of dbd plasma actuators *Journal of Electrostatics* (accepted 15.04.2011)
- [3] Kogelschatz U 2003 *Plasma Chemistry and Plasma Processing* **23** 1–46
- [4] Wagner H, Brandenburg R, Kozlov K, Sonnenfeld A, Michel P and Behnke J 2003 *Vacuum* **71** 417 – 436
- [5] Enloe C L, McLaughlin T E, VanDyken R D, Kachner K D, Jumper E J, Corke T C, Post M and Haddad O 2004 *AIAA Journal* **42** 595–604
- [6] Kriegseis J, Möller B, Grundmann S and Tropea C 2011 *AIAA-paper 2011-155*
- [7] Pavon S, Dorier J L, Hollenstein C, Ott P and Leyland P 2007 *J. Phys. D: Appl. Phys.* **40** 1733–1741
- [8] Barckmann K, Kriegseis J, Grundmann S and Tropea C 2010 *AIAA-paper 2010-4258*
- [9] Benard N, Balcon N and Moreau E 2008 *J. Phys. D: Appl. Phys.* **41** 042002 (5pp)
- [10] Versailles P, Gingras-Gosselin V and Vo H 2010 *AIAA Journal* **48** 859–863